Continuous measurement method and mathematical model for soil compactness

Huihui Zhao[1], Tao Cui[1,2], Li Yang[1,2], Qingyan Hou[3], Weijun Yan[3], Xiantao He[1,2], Chenlong Fan[1], Jiaqi Dong[1], Dongxing Zhang[1,2*]

(1. *College of Engineering, China Agricultural University, Beijing 100083, China*;
2. *The Soil-Machine-Plant Key Laboratory of the Ministry of Agriculture of China, Beijing 100083, China*;
3. *Shandong Guofeng Machinery Co., Ltd, Jining 272000, Shandong, China*)

Abstract: With the continuous improvement of agricultural mechanization, soil compaction becomes more and more serious. Serious soil compaction has been considered as an important negative factor affecting crop growth and yield. The measurement of soil compactness is a common method to measure the soil compaction level. In order to solve the problems of discontinuous sampling, time-consuming and poor real-time soil compactness measurement, a real-time measurement method of soil compactness based on fertilizing shovel was proposed, and the mathematical model between fertilizing shovel arm deformation and soil compactness was established. Based on the interaction mechanism between fertilizing shovel and soil, through the force analysis of fertilizing shovel, it was found that the deformation of fertilizing shovel arm was positively correlated with the sum of soil compactness (SSC) within the range of tillage depth. In order to verify the theoretical analysis results and the detection accuracy of strain gauge, the static bench test was carried out. The test results showed that the strain gauge signal for measuring the deformation of the fertilizing shovel arm was significantly correlated with the applied force. The fitting curve of the linear correlation coefficient was 0.999, the maximum detection error was 0.68 kg, and the detecting accuracy was within the tolerance of 0.57%. Through field orthogonal experiments with four working depths and four compaction levels, a mathematical model of the strain gauge signal and the SSC within the range of tillage depth was established. The experiment showed that compared with the other three depths, the linear correlation coefficient at the tillage depth of 5 cm (TD5) was the lowest, and the slope of the fitting curve was obviously different from the other three depths, so the 5 cm data were excluded when modeling. The model between mean signal value and mean SSC within the range of tillage depth was established based on the data of sampling points with tillage depths of 7.5 cm (TD7.5), 10 cm (TD10), and 12.5 cm (TD12.5). The linear correlation coefficient (R^2) of the model between mean signal value and mean SSC which eliminated 5 cm data was 0.980 and the root mean square error (RMSE) was 143.57 kPa. Compared with the linear model before averaging, the R^2 was improved by 8.65%, and the RMSE was reduced by 52.39%. This system can realize the real-time and continuous measurement of soil compactness and provide data support for follow-up intelligent agricultural operations.

Keywords: soil compactness measurement, fertilizing shovel, strain gauge, precision agriculture
DOI: 10.25165/j.ijabe.20221505.6707

Citation: Zhao H H, Cui T, Yang L, Hou Q Y, Yan W J, He X T, et al. Continuous measurement method and mathematical model for soil compactness. Int J Agric & Biol Eng, 2022; 15(5): 196–204.

1 Introduction

The soil may be crushed by the tires of agricultural machinery used in agricultural production operations, especially with the application and development of large machinery such as high-power tractors, combine harvesters, wide planters, etc. The compaction phenomenon could be increasingly serious, and once the soil compaction was formed, it will cause lasting damage[1-3]. Soil compactness is an important physical property of soil. It refers to the compaction degree of soil particles and is also known as soil hardness or soil penetration resistance. Serious soil compaction will cause difficulties in seed germination and emergence, and the growth of crop roots will be blocked, leading to crop yield reduction[4,5]. Soil compactness is not only related to the growth and development of crops but also related to the performance and energy consumption of agricultural machinery. Plowing or planting operations on compacted soil require more energy[6]. Therefore, the determination of soil compactness can provide data support and have an important guiding significance for the sustainable management and subsequent agricultural production of farmland[7].

It is difficult to directly measure the soil compactness in the farmland, so the soil compactness was generally acquired by measuring the cone index[8]. The American Society of Agricultural and Biological Engineers (ASABE) systematically

Received date: 2021-04-23 **Accepted date:** 2021-10-02
Biographies: Huihui Zhao, PhD candidate, research interest: intelligent control for maize precision planters, Email: zhaohh0220@163.com; **Tao Cui**, PhD, Associate Professor, research interest: full mechanization of maize production, Email: cuitao@cau.edu.cn; **Li Yang**, PhD, Professor, research interest: precision agriculture, Email: yangli@cau.edu.cn; **Qingyan Hou**, Engineer, research interest: full mechanization of maize production, Email: 187306957@qq.com; **Weijun Yan**, Engineer, research interest: full mechanization of maize production, Email: sdgfjx@126.com; **Xiantao He**, PhD, Associate Professor, research interest: precision agriculture and variable rate seeding technology, Email: hxt@cau.edu.cn; **Chenlong Fan**, PhD candidate, research interest: agricultural harvesting machinery monitoring and control technology, Email: fancl_nm@163.com;**Jiaqi Dong**, MS, research interest: intelligent control for precision planters, Email: 1170772523@qq.com.
***Corresponding author: Dongxing Zhang**, PhD, Professor, research interest: full mechanization of corn production. College of Engineering, China Agricultural University, No.17 Qinghua East Road, Haidian District, Beijing 100083, China. Tel: +86-10-62737765, Email: zhangdx@cau.edu.cn.

defined the soil cone index instrument and its operating method[9]. Cone index (CI) was defined as the quotient value of cone head resistance and cone head bottom area, which can characterize the depth of soil tillage layer and tillage resistance[10,11]. At present, there were two measurement methods of cone index[12]. One was the vertical cone penetrometer, which manually or mechanically penetrated the cone probe into the soil layer[13,14]. After years of development, the vertical cone penetrometer has made great breakthroughs and progress and is developing in the direction of diversification and compounding. The cone penetrometers frequently used were mostly handheld, mainly including the electronic cone index meter SC900 manufactured by Spectrum (USA) and the TJSD750 cone index meter by Top Company (China), which can simultaneously display soil compactness and measuring depth[15,16]. But it was difficult for the hand-held cone penetrometer to keep the constant speed of vertical penetration, which affected the measurement accuracy[17]. In order to solve this problem, some scholars developed a hydraulic or electric cone penetrometer, which used the motor or hydraulic system to drive the cone head into the soil at a constant speed, improving the measurement accuracy[18-21]. However, with the development of precision agriculture applications, there were higher requirements for real-time measurement. Both manual and mechanical cone penetrometers adopted point-by-point sampling measurement. When intensive sampling was carried out in large-scale site environment, the workload will be huge, and only the soil strength of discrete depths can be determined, which cannot meet the needs of precision agriculture development[22].

Therefore, scholars have proposed measurement methods based on horizontal probe penetrometers to realize the real-time dynamic and continuous measurement of soil compactness. Hemmat et al.[23,24] developed an integrated soil mechanical resistance sensor that can measure variation in soil strength in a 30 cm depth profile. The experiment results showed that the linear correlation coefficient between the measured value of the horizontal penetrometer and cone index was 0.75. Topakci et al.[7] designed a similar horizontal cone penetrometer. It can draw a soil resistance map with a soil depth of 40 cm on the spot by using the ArcGIS Kriging method. Alihamsyah et al.[25] developed two new horizontally operated penetrometers, a prismatic tip, and a tapered tip. The penetration resistance measured by two kinds of horizontal penetrometers had a good correlation with the penetration resistance measured by the Delmi penetrometer, the correlation coefficient was 0.742-0.988. Sun et al.[26,27] took the lead in using simplified impedance measurement technology to develop a combined horizontal penetrometer, which can simultaneously measure soil moisture content and soil firmness. And this penetrometer was enough sensitive to the spatial variability of soil compaction. Based on the principle of strain gauge force measurement, Liu et al.[28] developed a new embedded horizontal penetration soil compaction sensor. The cone head at the front of the cone penetrated into the soil and transmitted the soil resistance to the pressure sensor, which can effectively reflect the soil compaction. Zhao et al.[29] also designed a test system with tractor traction which can rapidly and continuously measure the farmland soil resistance. The tillage Resistance Index (TRI) value detected by the system can also reflect the soil compaction. All of the above studies showed that there was no significant correlation between the values measured by the horizontal penetrometer and the soil cone index (CI) at shallow operating depths. The relationship between the measured values of the horizontal penetrometer and the soil cone index (CI) was also related to the form of soil damage. The vertical penetrometer produced compressive damage to the soil. When the depth was shallow, the horizontal penetrometer will cause brittle damage to the soil, and the relationship between the two measurement methods was not significant. With the increase of the measuring depth, the soil brittle damage mode will change to the compression damage mode, which was consistent with the vertical penetrometer damage mode. The relationship between the two measurement methods became significantly correlated[23-24]. Therefore, the depth measured by the current horizontal penetrometer was generally greater than 30 cm, but the soil damage was serious after the measurement, which was not conducive to subsequent agricultural production. So, some scholars have chosen to measure the average soil compactness conditions in the depth range. Jia et al.[30] had used a displacement sensor to measure the expansion and contraction of the spokes of the press wheel and established a mathematical model between the sensor signal and the soil compactness. Experiments had shown that the spokes' expansion and contraction have a significant quadratic relationship with the average soil compactness of 0-20 cm, and the correlation coefficient was 99.8%. This provides us with a new method of measurement, which has important guiding significance for the decision-making of subsequent production operations.

In this study, in order to solve the problems that the existing soil compactness detection device had low detection accuracy, widespread soil damage, and could not directly carry out subsequent sowing operations after detection, a real-time measurement method of soil compactness was proposed based on fertilizing shovel to evaluate the overall soil compactness level within the tillage depth range, and realize the real-time dynamic measurement of soil compactness. Based on theoretical analysis, a model between the signal of the strain gauge and the sum of soil compactness (SSC) within the range of tillage depth was established by linear fitting method. And the model was evaluated by linear correlation coefficient (R^2) and root mean square error (RMSE).

2 Materials and methods

2.1 Fertilizing shovel

The fertilizing shovel (Figure 1) mainly comprises a core ploughshare furrow opener and a fertilizer guiding pipe. The core ploughshare furrow opener is a key component of the fertilizing shovel. And it is an acute-angle opener with a simple structure, good soil-entry performance, and a flat bottom of the trench. When the fertilizing shovel is working, its front edge and symmetrically curved surface make the soil rise along the curved surface, and throw stubble, surface dry soil clods, and weeds to both sides. The structure parameters are as follows: penetrating angle $\alpha = 39°$, clearance angle $\varepsilon = 4°$, chamfer angle $\gamma = 35°$, ploughshare height h=155 mm, ploughshare width B = 50 mm, shovel arm length L=700 mm, maximum tillage depth 15 cm.

2.2 Mechanical analysis of fertilizing shovel

As shown in Figure 2a, the fertilizing shovel was equivalent to a cantilever beam in operation. The tip of the fertilizing shovel was subjected to the resistance of the soil. Taking the tillage depth of 10 cm as an example, the force analysis of the fertilizing shovel was carried out to calculate the deformation of the strain gauge's sticking position.

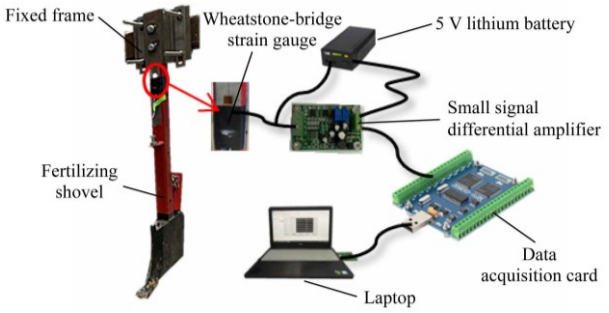

Figure 1 Schematic diagram of measuring device

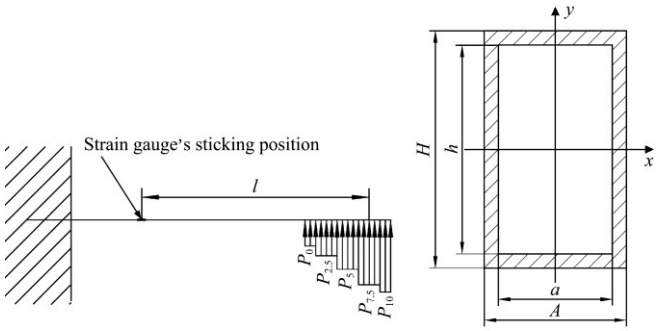

a. Force analysis of fertilizing shovel b. Cross section of fertilizing shovel arm

Note: l is the distance between the action point of the resultant force and the sticking position of the strain gauge, m; P_0 is the soil compactness at depth of 0 cm, kPa; $P_{2.5}$ is the soil compactness at depth of 2.5 cm, kPa; P_5 is the soil compactness at depth of 5 cm, kPa; $P_{7.5}$ is the soil compactness at depth of 7.5 cm, kPa; P_{10} is the soil compactness at depth of 10 cm, kPa. H is the width of fertilizer shovel arm, m; h is the inside width of cross section of fertilizer shovel arm, m; A is the external length of cross section of fertilizer shovel arm, m; a is the inside length of cross section of fertilizer shovel arm, m.

Figure 2 Force analysis of fertilizing shovel and cross section dimension parameters of fertilizing shovel arm

The bending moment of cross section at the sticking position of strain gauge was shown in Equation (1).

$$M = 0.025 \times \left(\frac{1}{2} P_0 + P_{2.5} + P_5 + P_{7.5} + \frac{1}{2} P_{10} \right) \times B \times l \quad (1)$$

where, M is the bending moment of the cross section at the sticking position of the strain gauge, kN·m; P_0 is the soil compactness at depth of 0 cm, kPa; $P_{2.5}$ is the soil compactness at depth of 2.5 cm, kPa; P_5 is the soil compactness at depth of 5 cm, kPa; $P_{7.5}$ is the soil compactness at depth of 7.5 cm, kPa; P_{10} is the soil compactness at depth of 10 cm, kPa; B is the width of fertilizer shovel, m; l is the distance between the action point of the resultant force and the sticking position of the strain gauge, m.

The shape and size parameters of the cross section of the fertilizing shovel arm were shown in Figure 2b, and the moment of inertia of the cross section on the z-axis can be calculated according to Equation (2).

$$I_z = \frac{1}{12(H \times A^3 - h \times a^3)} \quad (2)$$

where, I_Z is the moment of inertia of the cross section on the z-axis, m^4; H is the width of fertilizer shovel arm, m; h is the inside width of cross section of fertilizer shovel arm, m; A is the external length of cross section of fertilizer shovel arm, m; a is the inside length of cross section of fertilizer shovel arm, m.

The maximum stresses of the cross section and the strain of the fertilizing shovel at the sticking position were given by Equations (3) and (4).

$$\sigma_{\max} = \frac{My_{\max}}{I_z} \quad (3)$$

$$\varepsilon_{10} = \frac{My_{\max}}{E \times I_z \times 10^6} = \frac{25 \times lBy_{\max}}{E \times I_z \times 10^9} \left(\frac{1}{2} P_0 + P_{2.5} + P_5 + P_{7.5} + \frac{1}{2} P_{10} \right) = \frac{25 \times lBy_{\max}}{E \times I_z \times 10^9} P_{10sum} \quad (4)$$

where, $\sigma_{\max}$ is the maximum stress of the cross section of the fertilizing shovel at the sticking position, kPa; $y_{\max}$ is the farthest distance from the z-axis in the cross section, m; ε_{10} is the strain at the sticking position of the strain gauge when the depth of tillage is 10 cm; E is the elasticity modulus, GPa; P_{10sum} is the SSC within 10 cm of tillage depth, kPa.

It can be seen from Equation (4) that the strain measured by the strain gauge is related to the soil compactness at 0-10 cm, the sticking position of the strain gauge, and the position of the stress point. The soil compactness of the deeper part of the soil was greater than that of the shallow part. When the tillage depth was 10 cm, the position of the stress point should be within the range of 5-10 cm. But under different soil conditions, the values of P_0, $P_{2.5}$, P_5, $P_{7.5}$, P_{10} were different. And the stress points may be inconsistent, so it can assume that the stress point was at the position of 7.5 cm into the soil (the error of stress point position was within ±2.5 cm which can be ignored). If the sticking position of the strain gauge was farther from the shovel tip, the deformation on the surface of the shovel arm will become larger and easier to be detected. So the strain gauge was pasted below the fixed position.

When the sticking positions of the strain gauge and the stress point were determined, the strain measured by the strain gauge was related to the soil compactness at 0-10 cm.

2.3 Soil compactness measurement device and method

As shown in Figure 1, the soil compactness measurement device mainly includes fertilizing shovel, fixed frame, Wheatstone-bridge strain gauge (BF1K-3EB, China), 5 V lithium battery (5 V, 12600 mA, China), a small signal differential amplifier (AD620, China), data acquisition card (MPS-010602, China), PC laptop (DELL, USA).

The resistance value of the Wheatstone-bridge strain gauge is (1000±3) Ω, which is composed of four perpendicular resistors. The 502 glue was used to adhere the strain gauge to the upper end of the fertilizing shovel arm which had been polished in advance. The strain gauge outputted millivolt signal by detecting the deformation of fertilizing shovel arm, and the output voltage was amplified from millivolt to 0-5 V signal by a differential amplifier. The data acquisition card was connected to the upper computer laptop through USB, and had 16 channels of 0-10 V single ended analog signal input. When the amplified signal was connected to the analog signal interface of the acquisition card, the signal recording software based on LabVIEW can be used to collect the amplified signal. The acquisition frequency can be selected, up to 1000 Hz. The collected signal was saved in .txt format and imported into excel. The SSC within the range of tillage depth was calculated through the model calibrated in advance

2.4 Accuracy test of measurement device

From Equation (4) and the above analysis, it can be seen that the soil compactness within the range of tillage depth can be calculated by detecting the deformation of the fertilizing shovel arm. The deformation of fertilizing shovel arm was small, so the Wheatstone-bridge strain gauge sensitive to small deformation was selected to detect the deformation of fertilizing shovel arm. The deformation detected by the Wheatstone-bridge strain gauge was taken as the basis for evaluating the SSC within the range of tillage

depth. The detection accuracy of the measurement device must be ensured. When the depth was set at 10 cm, the resistance of the fertilizing shovel was replaced by the hanging weight. From 0 to 103.6 kg, with an interval of 10 kg, three bench tests of loading and unloading were carried out, and the amplified strain gauge signal was collected with the data acquisition card, as shown in Figure 3a. It can be seen that the relationship between the strain gauge signal and applied force was a linear positive correlation, and the linear correlation coefficient was as high as 0.999 (Figure 3b), which was consistent with the theoretical analysis results.

a. Bench test of measurement device

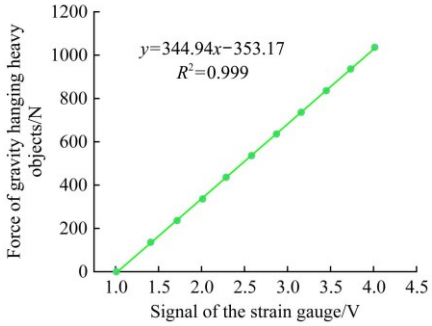

b. Results of the bench test

Figure 3 Bench test of measurement device and its results

Subsequently, a similar method was implemented but the above growing gradually hanging weight was replaced with different values, and the detecting accuracy of the measurement device was examined by comparing calculated force based on the above-mentioned relationship with actual force, illustrated in Figure 4. Through three replications, it turned out that the detecting accuracy of the measurement device was within the tolerance of 0.57% and the maximum detection error was 0.68 kg.

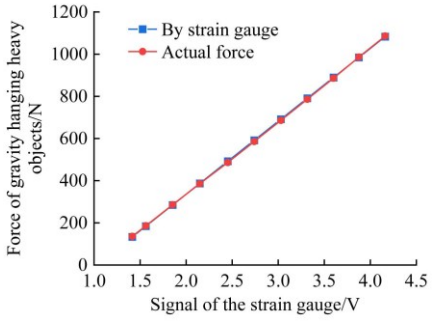

Figure 4 Discrepancy between the real and calculated forces

2.5 Model calibration experiment

2.5.1 Experiment arrangement

In order to establish a model between the SSC and the deformation signal of the fertilizing shovel arm, a model calibration experiment was carried out at a forward speed of 8 km/h. Four tillage depth levels and four compaction levels were set. The working depth of the fertilizing shovel was 0-15 cm. And according to the different fertilizer requirements of each growth period of maize, base fertilizer (fertilizing depth: 14-15 cm), topdressing (fertilizing depth: 8-10 cm) and seed fertilizer (fertilizing depth: 4-5 cm)[31,32], the four tillage depths of 5 cm (TD5), 7.5 cm (TD7.5), 10 cm (TD10) and 12.5 cm (TD12.5) were selected. The different soil compaction times (1 time (SCT1), 3 times (SCT3), 5 times (SCT5), and 10 times (SCT10)) were selected as four compaction levels. After 5 compaction times, the hardness variation of the soil was relatively small, so compaction 10 times was selected as the fourth compaction level. The test parameters are listed in Table 1.

Table 1 Test parameters and levels

Level	1	2	3	4
Tillage depth/cm	5.0	7.5	10.0	12.5
Soil compaction times	1	3	5	10

From Equation (4), the relationship between strain and soil compactness at TD5, TD7.5, and TD12.5 can be obtained. It was assumed that the stress points are 2.5 cm away from the tip of the shovel, the strains were shown in Equations (5)-(7), respectively.

$$\varepsilon_5=\frac{25lBy_{\max}}{E\times I_z\times10^9}\left(\frac{1}{2}P_0+P_{2.5}+\frac{1}{2}P_5\right)=\frac{25lBy_{\max}}{E\times I_z\times10^9}P_{5\text{sum}} \tag{5}$$

$$\varepsilon_{7.5}=\frac{25lBy_{\max}}{E\times I_z\times10^9}\left(\frac{1}{2}P_0+P_{2.5}+P_5+\frac{1}{2}P_{7.5}\right)=\frac{25lBy_{\max}}{E\times I_z\times10^9}P_{7.5\text{sum}} \tag{6}$$

$$\begin{aligned}\varepsilon_{12.5}&=\frac{25lBy_{\max}}{E\times I_z\times10^9}\left(\frac{1}{2}P_0+P_{2.5}+P_5+P_{7.5}+P_{10}+\frac{1}{2}P_{12.5}\right)\\&=\frac{25lBy_{\max}}{E\times I_z\times10^9}P_{12.5\text{sum}}\end{aligned} \tag{7}$$

where, $P_{12.5}$ is the soil compactness at depth of 12.5 cm, kPa; ε_5, $\varepsilon_{7.5}$ and $\varepsilon_{12.5}$ are the deformation at the sticking point of the strain gauge for TD5, TD7.5, and TD12.5, respectively; $P_{5\text{sum}}$, $P_{7.5\text{sum}}$, and $P_{12.5\text{sum}}$ are respectively the total level of soil compactness within the range of tillage depth for TD5, TD7.5, and TD12.5, kPa.

After the test, the strain gauge signal collected by the data acquisition card and the soil compactness data collected by the manual were compared and analyzed to obtain the relationship function between the two. Thus, the model between the two was established.

2.5.2 One-to-one correspondence of sampling position between manual and data acquisition card

During the experiment, due to the fluctuation of the tractor's driving speed, it was difficult to achieve a one-to-one correspondence of the sampling position between the data acquisition card and the manual. There was a certain position error between the two which led to the experimenting error. In order to solve this problem, in the test area, reflection strips were set up every 20 cm, and the soil compactness information of the position of the reflection strip was manually collected. The laser sensor was fixed on the frame of the three-point suspension machine. Also, the signal of the laser sensor and the strain gauge were collected together by the data acquisition card. When the laser light emitted by the laser sensor is swept through the reflective strips, the signal of the laser sensor will have a falling edge. According to the above method, the strain gauge signal sampled by the data acquisition card and the manual sampling were in the same position, which reduced the error caused by the uncertain position between the two. However, because of the natural sunlight, the laser sensor receiver could not receive the signal reflected by the reflector when the sunlight shone on the laser sensor, which might easily cause the failure of the laser sensor. Therefore, a laser sensor was installed at each end of the rack to

avoid the influence caused by the failure of one of them.

The width of the reflection strip was 5 cm. If the sampling frequency was too low, the data acquisition card may not be able to collect the falling edge signal of the laser sensor. Therefore, if the speed of the tractor was 8 km/h, Equations (8) and (9) can be used to calculate the minimum sampling frequency.

$$t = \frac{s}{v} = \frac{5\times10^{-2}}{8/3.6} = 2.25\times10^{-2}\ \text{s} \quad (8)$$

$$f = \frac{1}{t} = \frac{1}{2.25\times10^{-2}} = 44.44\ \text{HZ} \quad (9)$$

where, t is the time between the fertilizing shovel passing through the adjacent reflection strip, s; s is the width of the reflective strip, m; v is the tractor speed, m/s; f is the minimum sampling frequency, Hz.

According to the minimum sampling frequency of 44.44 HZ, the sampling frequency of the data acquisition card was selected as 100 HZ. Before the experiment, a preliminary experiment was carried out in the no-tillage field to verify the accuracy of the one-to-one correspondence method. The test results were shown in Figure 5. It can be seen that when the laser sensor swept the reflector, the data acquisition card can collect the sudden variation of the signal at the sampling frequency of 300 Hz. But the width between the adjacent falling edges was inconsistent, which indicated that the working speed did fluctuate in the forward process.

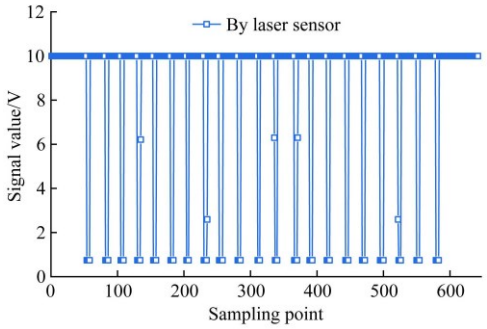

Figure 5 Laser sensor signal collected by data acquisition card

2.5.3 Experiment conditions

The model calibration experiments were implemented in Hebei Province. The soil texture was sandy loam, and the total test area was 60 m×10 m. Before the beginning of the experiment, the soil was treated with rotary tillage. Firstly, a rotary tiller was used to break the soil into small particles. Secondly, the soil was left in the air for two days to make the soil settle naturally. Thirdly, the soil was compacted by a roller with a width of 1.5 m, which met the experiment requirements. As shown in Figure 6, the fertilizing shovel was pulled forward by the three-point suspension at a constant speed of 8 km/h.

1. Tractor 2. Data acquisition card 3. Differential amplifier 4. Fertilizing shovel 5. Wheatstone-bridge strain gauge 6. Three-point suspension and frame 7. Compacted soil 8. Laser sensor 9: Reflection strips 10. Laptop

Figure 6 Components used in the experiments

As shown in Figure 7, each test area was mainly divided into three parts: acceleration area (5 m), test area (4 m), and deceleration area (5 m). Before the start of the experiment, reflection strips were set up every 20 cm next to the test area, and the tillage depth was adjusted to the specified tillage depth through a three-point suspension mechanism (Figure 8a). And at the position where the reflection strips were set up, the soil compactness data were collected manually every 20 cm by using the soil compactness meter. Each experimental plot had 20 sampling points. Specific operation was shown in Figure 8b, recording vertically seven values with an interval of 2.5 cm for 0-15 cm soil layer for each selected detecting point. After the test, the soil compactness data was exported through the software of the soil compactness meter.

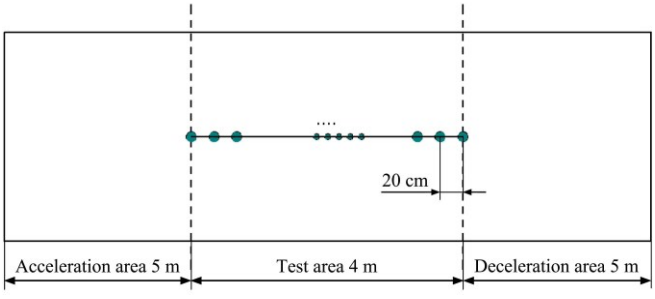

Figure 7 Experimental plot division

a. Tillage depth adjustment b. Manual sampling

Figure 8 Preparation before the experiment

3 Results and discussion

3.1 Relationship between signal value of the strain gauge and soil compactness measured manually at different depths

Linear fitting was carried out between the signal value of the strain gauge and the SSC within the range of tillage depth. And the linear fitting relationships at different depths were shown in Figure 9. At the condition of SCT1, SCT3, and SCT5, compared to SCT10, the data of the sampling points were more concentrated. This is because the number of compaction of SCT10 was 10 times, and the soil compactness was much greater than the other three levels.

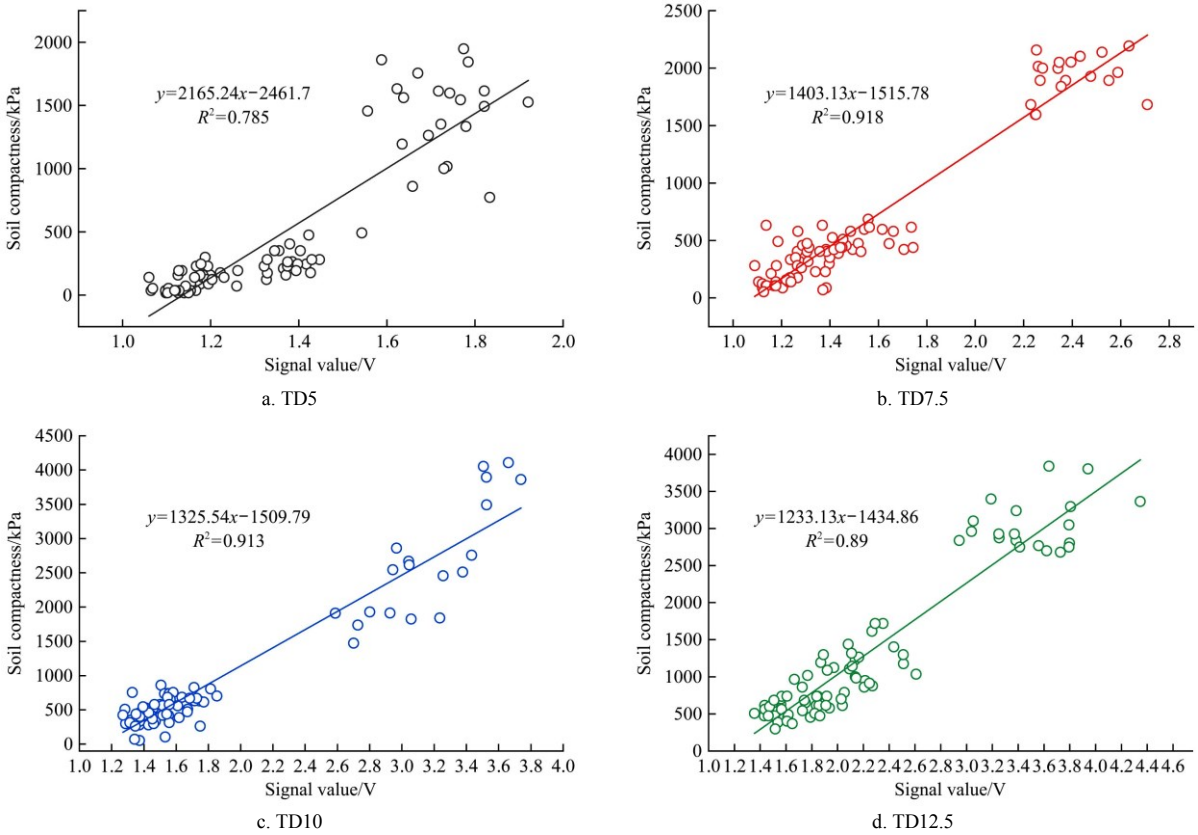

Note: TD5 means the tillage depth of 5 cm; TD7.5 means the tillage depth of 7.5 cm; TD10 means the tillage depth of 10 cm; TD12.5 means the tillage depth of 12.5 cm.

Figure 9 Relationship between signal value and manual measurement of soil compactness at different depths

In addition, for TD7.5, TD10, and TD12.5, the fitting R^2 were 0.918, 0.913, and 0.890, respectively, which were much higher than 0.785 of TD5. At TD5, the data points were more discrete. And under the condition of SCT1, SCT3, and SCT5, there was little difference in soil compactness at different compaction levels for TD5, and the SSC within the range of tillage depth was less than 500. That's probably because the SSC of tillage depth 5 cm was calculated by the soil compactness values of the three depths (P_0, $P_{2.5}$, and P_5), as shown in Equation (5). The resolution of the soil compactness meter is 35 kPa. When the surface compactness was collected in the soft soil, the difference in the soil compactness was small[9,33,34]. The soil compactness meter cannot distinguish accurately and had some errors.

In addition, as shown in Figure 9, the slopes of linear fitting curves at TD5, TD7.5, TD10, and TD12.5 were 2165.24, 1403.13, 1325.54, and 1233.13, respectively, showing a decreasing trend. This may be due to the increase in the number of compactions, a deeper soil compactness growth rate less than the soil compactness of the surface soil[35]. When the compaction reached a certain degree, the surface soil was firmer than the deep soil, which led to the upward movement of the force point and the declining slope of the fitting curve. For TD5, the slope was quite different from other tillage depths, and the fitting linear correlation coefficient was lower than the other three tillage depths. Therefore, when establishing the model between the SSC and the signal value of the strain gauge, the sampling point data with TD5 was eliminated.

3.2 Model establishment

The SSC within the range of tillage depth and the signal value of the strain gauge were modeled based on all sampling points. The fitting results are shown in Figure 10a. The R^2 was 0.875, and the RMSE was 322.12 kPa. From Figure 10a, it was found that a part of the data at TD5 was offset from the fitted curve, which is consistent with the conclusion in Section 3.1. It can be seen from Section 3.1 that the R^2 was found to be low for TD5. When the model was established, the data with TD5 should be eliminated. After eliminating the 5 cm data, the remaining sampling point data was used to refit the modeling. The fitting results were shown in Figure 10b.

As shown in Figure 10b, the linear correlation coefficient of the model was 0.902 and the RMSE was 301.58 kPa. Compared with the linear model before excluding the 5 cm data, the R^2 was improved by 3.1%, and the RMSE was reduced by 6.4%. It also reduced the degree of data dispersion. But as shown in Table 2, the slope and intercept of the linear curve did vary slightly. This could be due to seriously offset data which was only at the condition of SCT10 for TD5, and the offset sampling points were relatively small. Although the R^2 had been reduced, it had little effect on the slope and intercept of the overall fitted curve.

Take the average of the signal value and SSC of all sampling points in each test plot to obtain the mean signal value and the mean SSC under different treatments, as shown in Table 3. According to the above, 5 cm data was eliminated and linear fitting

was performed for all remaining points. The model of mean signal value and mean SSC of all sampling points (delete data of TD5) was shown in Equation (8).

$$f_P = 1277.9 f_s - 1422.4 \quad (8)$$

where, f_p is the SSC within the range of tillage depth, kPa; f_s is the amplified signal value of the strain gauge, V.

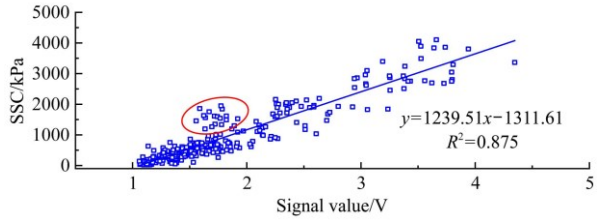

a. All sampling points

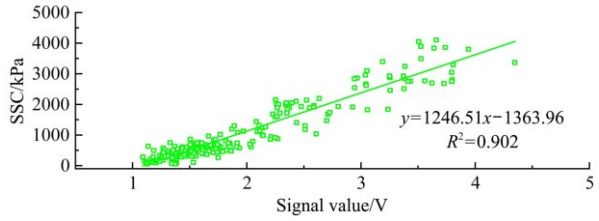

b. Delete data of TD5

Figure 10 Model establishment between the SSC within the range of tillage depth and signal value of the strain gauge

Table 2 Parameters of the two models

Parameter	All sampling point	Delete data of TD5
Slope	1239.5	1246.51
Intercept	−1311.61	−1363.96
Linear correlation coefficient	0.875	0.902
RMSE/kPa	322.12	301.58

Table 3 Statistics of mean signal value and mean SSC of field experiment

Tillage depth	Soil compaction time	Mean signal value/mV	Mean SSC/kPa
TD5	SCT1	1118.07	43.75
	SCT3	1203.51	168.45
	SCT5	1391.39	287.14
	SCT10	1724.56	1439.52
TD7.5	SCT1	1189.68	153.50
	SCT3	1318.70	359.10
	SCT5	1521.01	517.76
	SCT10	2395.55	1929.55
TD10	SCT1	1417.80	315.29
	SCT3	1468.09	532.33
	SCT5	1650.55	662.05
	SCT10	3160.75	2654.76
TD12.5	SCT1	1536.97	545.05
	SCT3	1856.17	736.40
	SCT5	2227.97	1202.48
	SCT10	3515.29	3044.30

Note: TD5 means the tillage depth of 5 cm; TD7.5 means the tillage depth of 7.5 cm; TD10 means the tillage depth of 10 cm; TD12.5 means the tillage depth of 12.5 cm; SCT1 means soil compaction 1 time; SCT3 means soil compaction 3 times; SCT5 means soil compaction 5 times; SCT10 means soil compaction 10 times; SSC means the sum of soil compactness.

As shown in Figure 11, the R^2 between the mean signal value and the mean SSC was 0.980, which had a high correlation and significance. And the RMSE was 143.57 kPa. Compared with the linear model before averaging, the R^2 was improved by 8.65%, and the RMSE was reduced by 52.39%. This showed that the variable soil compactness can be detected by the strain gauge and soil compactness level can be characterized by detecting the deformation of the fertilizing shovel arm. Therefore, the model between mean signal value and mean SSC of all sampling points (delete data of TD5) was taken as the final measurement model, which can improve the accuracy of measurement. In the practical application in the field, 20 signal values were collected continuously and the average value of 20 signal values was taken to calculate the SSC by the above model. Sun et al.[11,26] also made a linear fitting between the horizontal soil compactness value and the signal of the soil compactness meter at a depth of 15 cm, but the R^2 was only 51.3%. This is because Sun et al. used a horizontal penetrometer to measure the soil compactness at the depth of 15 cm. According to the research of Hemmat et al.[12,23-24], the soil compactness measured by the horizontal penetrometer showed a high correlation when the depth was more than 25 cm, and there was no significant correlation when the depth was 15 cm. However, the model in this study showed a high linear fit, which was due to the selection of the study on the overall soil compactness level within the range of tillage depth. Soil compactness was a synthetic index that characterized soil hardness and is closely related to soil resistance. When the fertilizing shovel operated in the field, the deformation of the fertilizing shovel arm was linearly related to the ditching resistance of the fertilizing shovel[11,36,37], so there was a significant linear relationship between the two. The establishment of the model can provide the basis for the follow-up work.

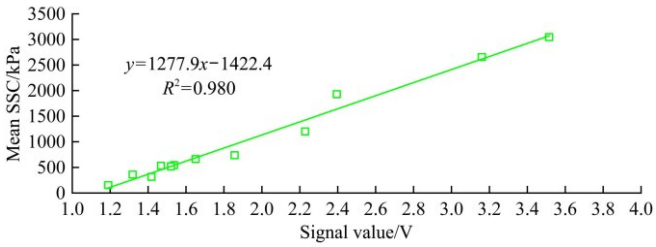

Note: SSC: The sum of soil compactness.

Figure 11 Linear fitting of mean signal and mean SSC of all sampling points (delete data of TD5)

3.3 Comprehensive analysis

The data of all sampling points were analyzed by analysis of variance (ANOVA) to determine the significance of compaction level, tillage depth, SSC within the range of tillage depth and their interaction on the signal value of the strain gauge, as well as determine the significance of compaction level, tillage depth and their interaction on the SSC within the range of tillage depth. The analysis results are listed in Table 4.

Table 4 ANOVA result of the contribution rate of each factor and interaction on signal value of the strain gauge and SSC

Factor	p-value of signal value	Significance	p-value of SSC	Significance
Soil compaction times (SCT)	0.000	***	0.000	***
Tillage depth (TD)	0.000	***	0.000	***
SSC	0.000	***	--	--
Compaction times×tillage depth	0.175	ns	0.000	***
Compaction times×SSC	0.998	ns	--	--
Tillage depth×SSC	0.614	ns	--	--

Note: "***" means $p \leq 0.001$; "**" means $p \leq 0.01$; "*" means $p \leq 0.05$; "ns" means no significant difference at 95% confidence interval; "--" means no significance analysis. '×' in this table represents the interaction between two factors.

The compaction times, tillage depth, and SSC had a significant effect on the signal value, but their interaction had no significant

effect on the signal value. The relationship between the mean signal value and the mean SSC under different treatments was shown in Figure 12. It can be clearly seen that the mean signal value of the strain gauge had increased with the increase of compaction level, tillage depth, and the mean SSC. Serious soil compaction will increase the resistance of the fertilizing shovel, resulting in the greater deformation of the fertilizing shovel arm and the increase of the signal of the strain gauge.

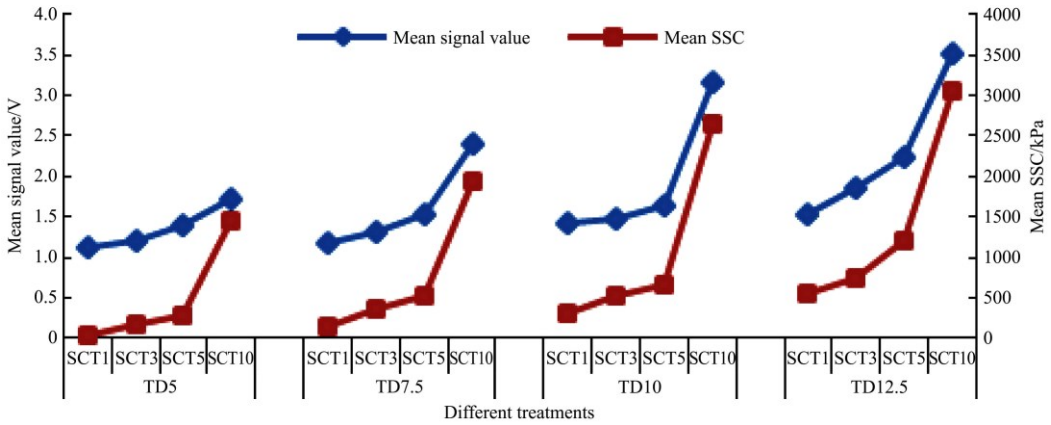

Figure 12 Mean signal value and mean SSC under different treatments

Table 4 also showed that the compaction level, tillage depth, and their interaction had a significant effect on the SSC of the sampling points. As shown in Figure 12, the mean SSC in each experimental plot increased with the increase of compaction level and tillage depth. With the continuous compaction of soil, the degree of soil compaction increased, and the value of SSC also increased. Under the same compaction level, it can be seen from Equations (4)-(7) that with the increase of tillage depth, the calculation of SSC was carried out with a deeper level of soil compactness superposition, resulting in the value of SSC of each sampling point increasing.

4 Conclusions

In this study, a new evaluation method of soil compactness level was proposed through the force analysis of the fertilizing shovel, and a real-time measuring device of soil compactness based on the deformation of the fertilizing shovel arm was developed, which can collect the signal of soil compactness continuously in real-time during the process of moving and solve the problems of time-consuming, discontinuous and poor real-time of the current soil compactness instrument. A model between SSC within the range of tillage depth and the signal value of the strain gauge was established through field experiments and verified the accuracy of the method. The supported conclusions can be drawn as follows:

1) Based on the static bench test, it was found that the strain gauge signal for detecting the deformation of the fertilizing shovel arm was highly linearly related to the applied force, and the linear correlation coefficient (R^2) was 0.999, which was consistent with the theoretical analysis results. The detecting accuracy of the measurement device was within the tolerance of 0.57%, and the maximum detection error was 0.68 kg, which met the design requirements.

2) Field experiments were carried out at a forward speed of 8 km/h. The 4 tillage depths (TD5, TD7.5, TD10, TD12.5) and 4 soil compaction treatments (SCT1, SCT3, SCT5, SCT10) were set as the experiment parameters and levels, respectively. The theoretical analysis results were verified, and the model of the strain gauge signal value and SSC within the range of tillage depth was established. The experimental results showed that the R^2 was poor when the tillage depth was 5 cm, and the slope of the fitting curve was quite different from the other three depths, so the 5 cm data was eliminated when modeling. The linear correlation coefficient (R^2) of the model between the mean signal value and mean SSC which eliminated 5 cm data was 0.980 and the root mean square error (RMSE) was 143.57 kPa. Compared with the linear model before averaging, the R^2 was improved by 8.65%, and the RMSE was reduced by 52.39%. The results show that the variable soil compactness can be detected by the strain gauge and soil compactness level can be characterized by detecting the deformation of the fertilizing shovel arm. Thus, the feasibility of the measuring method and device was verified.

Acknowledgements

This work was supported in part by the earmarked fund for CARS (CARS-02), the Soil-Machine-Plant Key Laboratory of the Ministry of Agriculture of China, and the Project of introducing talents in urgent need in Key Supporting Areas of Shandong Province in 2021.

[References]

[1] Li R S, Lin C H, Gao H W, Chen C L, Yuan Y L. The research of soil compaction caused by tractor. Transaction of the CSAM, 2002; 33(1): 126–129. (in Chinese)

[2] Keller T, Defossez P, Weisskopf P. Soilflex: A model for prediction of soil stresses and soil compaction due to agricultural field traffic including a synthesis of analytical approaches. Soil and Tillage Research, 2007; 93(2): 391–411.

[3] Li R S, Shi Y, Chi S Y, Su Y S. Soil compaction and tillage energy consumption caused by tires of agricultural machines. Transactions of the CSAM, 1999; 30(2): 13–17. (in Chinese)

[4] Batey T, Mckenzie D C. Soil compaction: Identification directly in the field. Soil Use Management, 2006; 22(2): 123–131.

[5] Chen G H, Weil R R. Root growth and yield of maize as affected by soil compaction and cover crops. Soil & Tillage Research, 2011; 117: 17–27.

[6] Adamchuk V I, Hummel J W, Morgan M T, Upadhyaya S K. On-the-go soil sensors for precision agriculture. Computers and Electronics in Agriculture, 2004; 44(1): 71–91.

[7] Topakci M, Unal I, Canakci M, Celik H K, Karayel D. Design of a horizontal penetrometer for measuring on-the-go soil resistance. Sensors, 2010; 10(10): 9337–9348.

[8] Canarache A. Factors and indices regarding excessive compactness of agricultural soils. Soil and Tillage Research, 1991; 19(2-3): 145–164.

[9] S313.3. Soil cone penetrometer. American Society of Agricultural and Biological Engineers (ASABE) standards, 2006.

[10] Luo X W, Zang Y, Zhou Z Y. Research progress in farming information acquisition technique for precision agriculture. Transactions of the CSAE,

2006; 22(1): 167–173. (in Chinese)
[11] Sun Y R, Ma D K, Lammers P S, Schmittmann O, Rose M. On-the-go measurement of soil water content and mechanical resistance by a combined horizontal penetrometer. Soil and Tillage Research, 2006; 86(2): 209–217.
[12] Hemmat A, Adamchuk V I. Sensor systems for measuring soil compaction: review and analysis. Computers and Electronics in Agriculture, 2008; 63(2): 89–103.
[13] Alihamsyah T, Humphries E G. On-the-go soil mechanical impedance measurements. In: Proceedings of the 1991 Symposium, ASAE, 1991; pp.300–306.
[14] Sirjacobs D, Hanquet B, Lebeau R, Destain M F. On-line soil mechanical resistance mapping and correlation with soil physical properties for precision agriculture. Soil and Tillage Research, 2001; 64: 231–242.
[15] Spectrum Technologies, Inc. Available: https://www.specmeters.com/brands/field-scout/sc900/. Accessed on [2021-04-23].
[16] Zhejiang Top Yunnong Technology Co., Ltd. Available: https://www.foodjx.com/st199351/product_5825925.html. Accessed on [2021-04-23].
[17] Yang C. Research on soil cone index of farmland design of measuring device. Master dissertation. Harbin: Northeast Agricultural University, 2019; 70p. (in Chinese)
[18] Alimardani R. Design and construction of a tractor mounted penetrometer. Journal of Agriculture & Social Sciences, 2005; 1(4): 297–300.
[19] Arriaga F J, Lowery B, Reinert D J, McSweeney K. Cone penetrometers as a tool for distinguishing soil profiles and mapping soil erosion. In: Hartemink A, Minasny B (Ed.). Digital Soil Morphometrics. Progress in Soil Science, Springer, 2016; pp.401–410. doi: 10.1007/978-3-319-28295-4_25.
[20] Meng F J, Ma D K, Sun Y R. Penetrometer with ball screw transmission. Transactions of the CSAM, 2009; 40(5): 52–55. (in Chinese)
[21] Li Y D. Experimental study on soil penetration resistance characteristics and design of testing device. Master dissertation. Harbin: Northeast Agricultural University, 2017; 73p. (in Chinese)
[22] Naderi-Boldaji M, Alamooti M Y, Sharifi A, Jamshidi B, Abbasi F, Minaee S. A combined sensor for on-the-go measurement of soil water content and mechanical resistance: Moisture sensor design and calibration. In: International Conference on Agricultural Engineering-AgEng, 2010; pp.163–170.
[23] Hemmat A, Adamchuk V I, Jasa P. Use of an instrumented disc coulter for mapping soil mechanical resistance. Soil and Tillage Research, 2008; 98(2): 150–163.
[24] Hemmat A, Khorsandy A, Masumi A A, Adamchuk V I. Influence of failure mode induced by a horizontally operated single-tip penetrometer on measured soil resistance. Soil & Tillage Research, 2009; 105(1): 49–54.
[25] Alihamsyah T, Humphries E G, Bowers C G. A technique for horizontal measurement of soil mechanical impedance. Transactions of the ASAE, 1990; 33(1): 73–77.
[26] Sun Y, Lammers P S, Ma D. Evaluation of a combined penetrometer for simultaneous measurement of penetration resistance and soil water content. Journal of Plant Nutrition and Soil Science, 2004; 167(6): 745–751.
[27] Sun Y R, Lammers P S, Ma D K, Lin J H, Zeng Q M. Determining soil physical properties by multi-sensor technique. Sensors and Actuators A: Physical, 2008; 147(1): 352–357.
[28] Liu J, Ma D K, Zeng Q M, Sun Y R. A real-time measuring system of soil compaction. Journal of China Agricultural University, 2007; 6: 71–74, 92. (in Chinese)
[29] Zhao X, Luo X W, Wells L G. Test of a continuously measure soil resistance system on farmland. Journal of Agricultural Mechanization Research, 2012; 34(8): 111–115. (in Chinese)
[30] Jia H L, Li Y, Qi J T, Fan X H, Wang W J, Guo M Z. Design and test of soil compaction acquisition system for sowing line surface based on ZigBee. Transactions of the CSAM, 2015; 46(12): 39–46, 61. (in Chinese)
[31] Wang Y X, Liang Z J, Cui T, Zhang D X, Qu Z, Yang L. Design and experiment of layered fertilization device for corn. Transactions of the CSAM, 2016; 47(S1): 163–169. (in Chinese)
[32] Xue S P, Zhu R X, Lei S W, Xue H L. Development of the combined layered fertilizing-seeding ditcher. Journal of Northwest A&F University: Natural Science Edition, 2008; 36(8): 223–228. (in Chinese)
[33] ASAE S313.3 FEB04. Soil cone penetrometer, 1998.
[34] Goutal N, Keller T, Défossez P, Ranger J. Soil compaction due to heavy forest traffic: measurements and simulations using an analytical soil compaction model. Annals of Forest Science, 2013; 70(5): 545–556.
[35] Arvidsson J, Westlin H, Keller T, Gilbertssonb M. Rubber track systems for conventional tractors-effects on soil compaction and traction. Soil and Tillage Research, 2011; 117: 103–109.
[36] Zhao Z J, Han C J, Guo H, Zhang J, Huang Q H, Yang W Z. Continuous measurement system design of soil mechanical resistance based on arduino. Agricultural Engineering, 2015; 5(4): 55–57, 62.
[37] Mouazen A M, Anthonis J, Saeys W, Ramon H. An automatic depth control system for on line measurement of spatial variation in soil compaction, part 1: Sensor design for measurement of frame height variation from soil surface. Biosystems Engineering, 2004; 89(2): 139–150.